Resonance Raman Spectra of the Polynuclear Complexes Ruthenium Red, Ruthenium Brown, and the Related 1,2-Diaminoethane Substituted Complexes

By **Jeremy R. Campbell** and **Robin J. H. Clark**, Christopher Ingold Laboratories, University College, London WC1H 0AJ
William P. Griffith * and **Jonathan P. Hall**, Inorganic Chemistry Research Laboratories, Imperial College, London SW7 2AY

The resonance Raman spectra of salts of ruthenium red, $[Ru_3O_2(NH_3)_{14}]^{6+}$, and ruthenium brown, $[Ru_3O_2(NH_3)_{14}]^{7+}$, in their normal, ^2H-, ^{15}N-, and ^{18}O-substituted forms have been measured using excitation in the 417—647 nm range. Similar measurements were carried out for the 1,2-diaminoethane-substituted analogues $[Ru_3O_2(NH_3)_{10}(en)_2]^{6+}$, $[Ru_3O_2(NH_3)_{10}(en)_2]^{7+}$, and their deuteriates. The a_{1g} and some of the a_{2u} fundamentals of these cations have been assigned and force-constant calculations on these modes carried out. The excitation profiles of the a_{1g} fundamentals have maxima close to the intense peaks, which lie between 18 400 and 21 800 cm^{-1}, in the electronic absorption spectra of these ions, and this information, together with Raman depolarisation data, lead to assignments for the resonant electronic transition in each case.

THE complex known as ruthenium red, made by aerobic oxidation of solutions of ruthenium trichloride in aqueous ammonia, has long been known [1] and is extensively used as a cytological reagent for visualising the ultrastructure of cell walls in optical and electron microscopy.[2] Recently, much work has been carried out on the ability of the ruthenium red cation to block those sites in biological tissue to which calcium ions normally bind.[3] The formulation in 1961 of ruthenium red as a trinuclear oxo-bridged species [4] has now been confirmed by an *X*-ray study on $[Ru_3O_2(NH_3)_{14}][S_2O_3]_3{\cdot}4H_2O$.[5]

The intense colour of ruthenium red arises from the very strong electronic absorption at 18 620 cm^{-1} (537 nm, ε 6.99 $\times$ 10^4 dm^3 mol^{-1} cm^{-1}); the related complex $[Ru_3O_2(NH_3)_{10}(en)_2]^{6+}$ (en = 1,2-diaminoethane) has a similar strong band [18 420 cm^{-1} (543 nm), ε 8.18 $\times$ 10^4 dm^3 mol^{-1} cm^{-1}] as do the oxidised species $[Ru_3O_2(NH_3)_{14}]^{7+}$ [21 790 cm^{-1} (459 nm), ε 4.38 $\times$ 10^4 dm^3 mol^{-1} cm^{-1}] and $[Ru_3O_2(NH_3)_{10}(en)_2]^{7+}$ [21 100 cm^{-1} (474 nm), ε 4.61 $\times$ 10^4 dm^3 mol^{-1} cm^{-1}].[6] These ions are clearly suitable subjects for resonance Raman studies, and indeed we find that they all give rich spectra. In order to help to assign the observed Raman bands we have also measured the spectra of the isotopically substituted species $[Ru_3O_2(N^2H_3)_{14}]^{6+}$, $[Ru_3O_2(N^2H_3)_{14}]^{7+}$, $[Ru_3O_2(^{15}NH_3)_{14}]^{6+}$, $[Ru_3O_2(^{15}NH_3)_{14}]^{7+}$, $[Ru_3{}^{18}O_2(NH_3)_{14}]^{6+}$, $[Ru_3{}^{18}O_2(NH_3)_{14}]^{7+}$, $[Ru_3{}^{18}O_2(N^2H_3)_{14}]^{6+}$, and $[Ru_3{}^{18}O_2(N^2H_3)_{14}]^{7+}$. During the course of our work a study utilising the resonance Raman spectra of ruthenium red as a probe for investigating the binding capacity of the complex to various sites was published, but no assignments for the bands were given.[7] In this paper we propose assignments for the Raman bands of these complexes and present a simple force-constant treatment of the results. Studies are also presented of the resonance Raman spectra of the related complexes $[Ru_3O_2(NH_3)_{10}(en)_2]^{6+}$, $[Ru_3O_2(N^2H_3)_{10}\{[^2H_4]en\}_2]^{6+}$, $[Ru_3O_2(NH_3)_{10}(en)_2]^{7+}$, and $[Ru_3O_2(N^2H_3)_{10}\{[^2H_4]en\}^2]^{7+}$ ($\{[^2H_4]en\}$ = the en ligand with four deuterium atoms on the amino-groups). Finally, detailed consideration of the excitation profiles of the a_{1g} Raman bands of the ions together with depolarisation ratios of these bands lead to a reasonable assignment for the resonant electronic bands within the framework of a proposed molecular-orbital scheme of bonding.

EXPERIMENTAL

Tetradeca-amminedi-μ-oxo-triruthenium Hexachloride Tetrahydrate.—The complex $[Ru_3O_2(NH_3)_{14}]Cl_6{\cdot}4H_2O$ (subsequently referred to as ruthenium red) was prepared by aerial oxidation of $RuCl_3{\cdot}3H_2O$–aqueous ammonia according to the literature method.[4] The salt was purified by repeated recrystallisation from 0.5 mol dm^{-3} ammonia solution at 60 °C and further purified by addition of a small amount of saturated sodium chloride solution to a saturated solution of the complex. Final yield of red-brown product 10% (Found: H, 5.1; Cl, 25.7; N, 22.7. $H_{50}Cl_6N_{14}O_6Ru_3$ requires H, 5.9; Cl, 24.8; N, 22.9%).

The *thiosulphate tetrahydrate* was prepared by addition of sodium thiosulphate solution to a solution of the chloride in 3 : 1 molar proportions. It forms iridescent green crystals (red by transmitted light) (Found: H, 4.7; N, 20.0; S, 19.8. $H_{50}N_{14}O_{15}Ru_3S_6$ requires H, 5.1; N, 20.0; S, 19.6%).

Isotopically Enriched Forms of Ruthenium Red.—$[Ru_3O_2(N^2H_3)_{14}]Cl_6$. Repeated evaporation to dryness of a solution of $[Ru_3O_2(NH_3)_{14}]Cl_6$ in heavy water in the presence of a little N^2H_3 gave the deuteriated product; its Raman spectrum was measured in ^2H_2O solution.

$[Ru_3O_2(^{15}NH_3)_{14}]Cl_6$. A small-scale version of the literature preparation [4] of ruthenium red was used, $^{15}NH_3$ solutions being used in place of aqueous $^{14}NH_3$. Such solutions were made by addition of aqueous sodium hydroxide to $^{15}NH_4Cl$ (98.6% ^{15}N), collection of the $^{15}NH_3$ in a cold trap, and dissolution in water.

$[Ru_3{}^{18}O_2(NH_3)_{14}]^{6+}$. To a solution of ammonia in $H_2{}^{18}O$ (99.5% isotopically enriched) was added $[Ru(NH_3)_5Cl]Cl_2$ (prepared as in ref. 8) and this was held at 75 °C under a 10% $^{18}O_2$ (99% isotopic enrichment)–90% N_2 atmosphere for 6 h before evaporating to dryness *in vacuo*. The resonance Raman spectra of a solution of this material in H_2O and in $H_2{}^{18}O$ were identical, suggesting that no significant exchange of bridged oxo-ligands with $H_2{}^{16}O$ occurs at room temperature.

$[Ru_3{}^{18}O_2(N^2H_3)_{14}]^{6+}$. This was made in the same manner as the preceding preparation, N^2H_3 replacing NH_3.

Tetradeca-amminedi-μ-oxo-triruthenium Heptachloride

Tetrahydrate.—The complex $[Ru_3O_2(NH_3)_{14}]Cl_7 \cdot 4H_2O$ (subsequently referred to as ruthenium brown) was prepared as follows. Ruthenium red (0.7 g in 100 cm^3 water) was oxidised in hydrochloric acid (5 cm^3, 2 mol dm^{-3}) by hydrogen peroxide (25 cm^3, 30%). After warming to 50 °C for 1 h, the brown powder was collected by filtration from the cooled solution. Yield 0.5 g (70%) (Found: H, 5.6; Cl, 27.8; N, 21.9. $H_{50}Cl_7N_{14}O_6Ru_3$ requires H, 5.5; Cl, 27.6; N, 21.6%).

Isotopically Enriched Forms of Ruthenium Brown.—The complexes $[Ru_3O_2(N^2H_3)_{14}]^{7+}$, $[Ru_3O_2(^{15}NH_3)_{14}]^{7+}$, $[Ru_3{}^{18}O_2(NH_3)_{14}]^{7+}$, and $[Ru_3{}^{18}O_2(N^2H_3)_{14}]^{7+}$ were made by the *in situ* oxidation of the corresponding ruthenium red species by addition of a little 2 mol dm^{-3} hydrochloric acid and 30% hydrogen peroxide or (in the case of the ^{15}N and ^{18}O species), ceric ammonium nitrate, $[NH_4]_2[Ce(NO_3)_6]$. Solid $[Ru_3O_2(N^2H_3)_{14}]Cl_7 \cdot 4^2H_2O$ was made by evaporation of the solution in ^2H_2O.

Ethylenediamine Substituted Products.—Deca-amminebis(1,2-diaminoethane)di-μ-oxo-triruthenium hexachloride, $[Ru_3O_2(NH_3)_{10}(en)_2]Cl_6$. Green needles of the complex were obtained from an aqueous solution of ruthenium red and 1,2-diaminoethane, following the literature procedure.[9] Yield 80% (Found: C, 5.0; H, 5.7; Cl, 25.4: N, 23.3. $C_4H_{46}Cl_6N_{14}O_2Ru_3$ requires C, 5.7; H, 5.5; Cl, 25.4; N, 23.4%).

The deuteriated form, $[Ru_3O_2(N^2H_3)_{10}\{[^2H_4]en\}_2]Cl_6$ was made in the same fashion as deuteriated ruthenium red.

Deca-amminebis(1,2-diaminoethane)di-μ-oxo-triruthenium heptachloride, $[Ru_3O_2(NH_3)_{10}(en)_2]Cl_7$. The normal and deuteriated $\{[Ru_3O_2(N^2H_3)_{10}\{[^2H_4]en\}_2]Cl_7\}$ forms of this complex were prepared from $[Ru_3O_2(NH_3)_{10}(en)_2]Cl_6$ by a procedure analogous to that used to obtain ruthenium brown derivatives from ruthenium red.

Raman spectra were recorded on Spex 1401, 14018 (R5), and 14018 (R6) double monochromator instruments. Exciting radiation was provided by Coherent Radiation models 52 (Kr^+) and CR12 (Ar^+) lasers, the latter in conjunction with a model 490 dye laser using sodium fluorescein and stilbene-3 dyes. Aqueous solutions of the complexes were held in rotating glass cells to avoid local heating effects. Band intensities were measured relative to the $\nu_1(a_1)$ band of SO_4^{2-} (as potassium sulphate) and corrected for the spectral response of the instrument. Spectra of solids were measured in KCl discs which were then spun.

Infrared spectra were measured on Perkin-Elmer 225 and 597 instruments, samples being pressed into alkali halide discs and also run as Nujol mulls between caesium iodide plates.

Electronic spectra were measured on Perkin-Elmer 402 and 551 instruments (aqueous solutions) and on a Cary 14 spectrometer for the transmission spectra of alkali halide discs.

RESULTS

The resonance Raman spectra of ruthenium red, ruthenium brown, and the 1,2-diaminoethane analogues are reproduced in Figure 1, and the vibrational wavenumbers listed in Tables 1—3, while i.r. data are presented in Table 4. Data on isotopically substituted species are also given in the Tables.

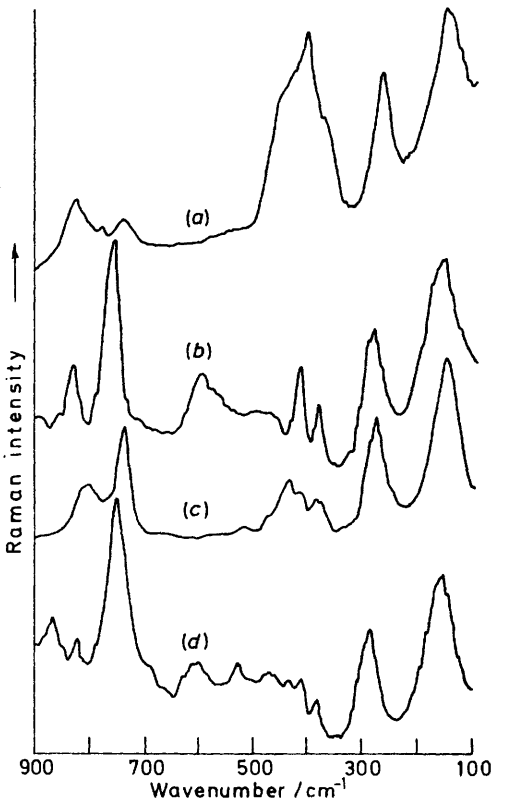

FIGURE 1 Resonance Raman spectra for (*a*) $[Ru_3O_2(NH_3)_{14}]^{6+}$; (*b*) $[Ru_3O_2(NH_3)_{14}]^{7+}$; (*c*) $[Ru_3O_2(NH_3)_{10}(en)_2]^{6+}$; (*d*) $[Ru_3O_2(NH_3)_{10}(en)_2]^{7+}$ in aqueous solution (5×10^{-5} mol dm^{-3}). Exciting radiation: 18 836 cm^{-1} (530.9 nm) for (*a*) and (*c*), and 21 000 cm^{-1} (476.2 nm) for (*b*) and (*d*)

TABLE 1

Resonance Raman spectra of ruthenium red, $[Ru_3O_2(NH_3)_{14}]^{6+}$ [a]

	Wavenumbers/cm^{-1}											
$[Ru_3O_2(NH_3)_{14}]Cl_6 \cdot 4H_2O$ [b]	816 (3)		744 (4)	744 (4)		477 (3)	446 (5)	408 (10)	375 (6)	281 (8)	168 (9)
$[Ru_3O_2(NH_3)_{14}]^{6+}$	827 (4)	778 (2)	742 (4)	742 (4)	545 (½)	474 (2)	443 (5)	413 (10)	370 (2)	274 (8)	150 (8)
p [c]	0.30		0.24	0.24			0.32	0.28	0.30	0.27	0 26
$[Ru_3O_2(N^2H_3)_{14}]^{6+}$	825 (3)	759 (2)	705(3)	615 (1)	534 (—)	450 (2)	428 (5)	400 (9)	354 (2)	250 (10)	144 (6)
$[Ru_3O_2(^{15}NH_3)_{14}]^{6+}$	826 (3)	783 (1)	731 (2)	731 (2)		457 (2)	430 (7)	406 (10)	370 (2)	270 (4)	150 (5)
$[Ru_3{}^{18}O_2(NH_3)_{14}]^{6+}$	786 (4)	739 (1)	710 (2)	710 (2)	546 (½)	475 (1)	442 (4)	397 (10)	362 (2)	274 (5)	151 (5)
$[Ru_3{}^{18}O_2(N^2H_3)_{14}]^{6+}$	780 (4)	718 (1)	676 (4)	615 (2)	523 (½)	443 (2)	409 (5)	384 (10)	338 (2)	246 (10)	144 (6)
Assignment	ν(RuO)			$\rho(N_{eq}H_3)$		$\nu(RuN_{eq})$	$\nu(Ru'N')$	$\nu(RuN_{ax})$		$\delta(ORuN_{eq})$	ν(RuO)
	ν_1					ν_2	ν_3	ν_4		ν_5	ν_6

[a] Relative intensities are given in parentheses. [b] Solid state spectra. All other data relate to aqueous solutions. [c] *p* = Depolarisation ratio at resonance.

Resonance Raman spectra were measured in the range 60—1 200 cm^{-1} using excitation in the range 417—647 nm on aqueous solutions, usually 5×10^{-5} mol dm^{-3} (data on the solids were obtained over the same ranges). A typical intensity enhancement for ruthenium red is 50-fold from 647.1 nm excitation (well clear of the electronic absorption

TABLE 2

Resonance Raman spectra of ruthenium brown $[Ru_3O_2(NH_3)_{14}]^{7+}$ *

	Wavenumbers/cm^{-1}										
$[Ru_3O_2(NH_3)_{14}]Cl_7 \cdot 4H_2O$ [b]	895 (½)	810 (2)	745 (4)	745 (4)	550 (1)	480 (1)	450 (1)	428 (3)	373 (2)	275 (6)	155 (10)
$[Ru_3O_2(NH_3)_{14}]^{7+}$	898 (1)	829 (6)	761 (10)	761 (10)	599 (3)	469 (2)	443 (2)	424 (9)	385 (3)	281 (8)	157 (9)
p		0.26	0.28	0.28	0.31		0.44	0.28	0.58	0.31	0.38
$[Ru_3O_2(N^2H_3)_{14}]^{7+}$	856 (1)	803 (3)	730 (9)	562 (5)	562 (5)	458 (2)	428 (2)	405 (4)	368 (3)	258 (10)	154 (6)
			770 (5)								
$[Ru_3O_2(^{15}NH_3)_{14}]^{7+}$	887 (1)	816 (3)	738 (5)	738 (5)		454 (2)	obsc.	413 (10)	371 (4)	270 (2)	155 (3)
$[Ru_3{}^{18}O_2(NH_3)_{14}]^{7+}$	880 (1)	795 (2)	728 (7)	728 (7)	598 (2)	467 (½)		403 (5)	365 (2)	282 (6)	156 (10)
$[Ru_3{}^{18}O_2(N^2H_3)_{14}]^{7+}$	840 (½)	778 (2)	710 (3)	569 (2)	569 (2)	460 (1)	423 (3)	401 (10)	349 (1)	253 (6)	153 (4)
Assignment		ν(RuO)		$\rho(N_{eq}H_3)$		$\nu(RuN_{eq})$	ν(Ru'N')	$\nu(RuN_{ax})$		$\delta(ORuN_{eq})$	ν(RuO)
		ν_1				ν_2	ν_3	ν_4		ν_5	ν_6

* See footnotes to Table 1.

maximum of the complex, giving an off-resonance spectrum) to 530.9 nm excitation (which is on resonance). Allowing for differences in concentrations, the Raman bands of ruthenium red are some 10^4 times more intense than the ν_1 band of the sulphate ion used as an internal standard, so there is certainly a strong resonance effect.

It was observed that the 413 cm^{-1} band in particular is sensitive to addition of ions such as sulphate, shifting to 397 cm^{-1} in 0.1 mol dm^{-3} SO_4^{2-}; all bands increase in intensity and some change their relative intensities in the presence of sulphate ion. The electronic spectrum of ruthenium red is known to be affected by added ions, the 18 620 cm^{-1} absorption band shifting slightly and becoming stronger.[10] It is likely therefore that the shifts observed in the 413 cm^{-1} band [7] when ruthenium red is attached to those sites in biological material which normally bind calcium ion are in some way due to electrostatic forces at such sites.

TABLE 3

Resonance Raman spectra of 1,2-diaminoethane derivatives, $[Ru_3O_2(NH_3)_{10}(en)_2]^{n+}$ (n = 6 or 7) *

$[Ru_3O_2(NH_3)_{10}(en)_2]Cl_6$		814 (1)	790 (1)	736 (2)		570 (½)	530 (½)	470 (½)	427 (2)	427 (2)		368 (4)	283 (4)	156 (10)
			760 (½)				510 (½)					312 (1)	240 (1)	
$[Ru_3O_2(NH_3)_{10}(en)_2]^{6+}$	*p*	810 (3)	770 (1)	744 (6)		575 (½)	521 (1)	474 (1)	437 (6)	410 (3)	391 (2)	374 (2)	279 (7)	152 (10)
		0.33		0.26				0.25	0.28	0.29	0.27	0.28	0.27	0.27
$[Ru_3O_2(N^2H_3)_{10}\{[^2H_4]en\}_2]^{6+}$		798 (2)	750 (1)	616 (½)		556 (½)	505 (½)	442 (1)	400 (2)	380 (1)	354 (1)	354 (1)	253 (10)	146 (10
			706 (3)											
$[Ru_3O_2(NH_3)_{10}(en)_2]Cl_7$ [b]	855 (3)	815 (3)	760 (7)	760 (7)	690(1)	590 (1)	530 (2)	470 (1)	428 (4)	410 (1)		375 (4)	282 (7)	160 (10)
			740 (7)	740 (7)				450 (2)						
$[Ru_3O_2(NH_3)_{10}(en)_2]^{7+}$		870 (3)	820 (1)	754 (8)	690 (1)	603 (2)	527 (1)	460 (1)	435 (1)	412 (1)		381 (2)	289 (6)	157 (10)
	p		0.33	0.31	0.35	0.22						0.26	0.27	0.36
$[Ru_3O_2(N^2H_3)_{10}\{[^2H_4]en\}_2]^{7+}$		848 (1)	798 (1)	736 (10)	562 (3)	562 (3)	492 (2)	440 (2)	422 (2)	400 (2)		365 (2)	263 (10)	150 (8)
Assignment			ν(RuO)		$\rho(N_{eq}H_3)$			$\nu(RuN_{eq})$	ν(Ru'N')	$\nu(RuN_{ax})$			$\delta(ORuN_{eq})$	ν(RuO)
			ν_1					ν_2	ν_3	ν_4			ν_5	ν_6

* See footnotes to Table 1.

DISCUSSION

Structure of the Complexes.—Structural data are available for $[Ru_3O_2(NH_3)_{14}][S_2O_3]_3 \cdot 4H_2O$ and for $[Ru_3O_2(NH_3)_{10}(en)_2]Cl_6$ only, though chemical,[4] polarographic, and electronic spectral data [6] suggest that ruthenium brown has a very similar structure to that of ruthenium red.

In the thiosulphate salt of ruthenium red [5] there is an essentially linear N–Ru–O–Ru–O–Ru–N backbone, the bridging oxo-ligands (Ru–O 1.845—1.857 Å) and ammine ligands (Ru–N 2.087—2.172 Å) conferring octahedral co-ordination on the metal atoms. An unexpected feature of the structure of the anion is that one terminal RuN_4 unit has a dihedral angle of 31° with respect to the other two (central and terminal) RuN_4 units, this latter pair being essentially eclipsed. Thus the structure is akin to that in Figure 2(*a*), where the dihedral angle is illustrated as being 45°. If we neglect the protons or assume free rotation of NH_3 groups about each Ru–N axis the effective symmetry of the cation is C_4. In an idealised form of this structure, which could perhaps be that present in solution, in which the dihedral angle is 45° [Figure 2(*a*)], the symmetry would be C_{4v}.

TABLE 4

Infrared band maxima (cm^{-1}) of ruthenium red, ruthenium brown, and their 1,2-diaminoethane analogues (sp = sharp)

$[Ru_3O_2(NH_3)_{14}]Cl_6 \cdot 4H_2O$ [a]	845 (sh), 805s, 753m, 670w	560vw, 520w	470vw, 450m,sp, 425w	318m,sp, 260s, 241, 200
$[Ru_3O_2(N^2H_3)_{14}]Cl_6 \cdot 4^2H_2O$	780 (sh), 798s, 650m, 630w	565w, 525w	447 (sh), 427ms	300s,sp, 260 (sh), 230s
$[Ru_3O_2(NH_3)_{14}]Cl_7 \cdot 4H_2O$	845s, 710mw	580w, 535w	478m, 418w	305 (sh), 280ms
$[Ru_3O_2(N^2H_3)_{14}]Cl_7 \cdot 4^2H_2O$	820 (sh), 800ms, 650m	558w	452m, 402w	260 (sh), 230ms
$[Ru_3O_2(NH_3)_{10}(en)_2]Cl_6$ [b]	825m, 800ms, 785s, 753vw, 700vw	548m	473s, 436ms, 401w	318s,sp, 270s, 230, 170, 154
$[Ru_3O_2(N^2H_3)_{10}\{[^2H_4]en\}_2]Cl_6$	808ms, 778m, 675vw, 641mw, 610mw	573vw, 530vw	448m, 443 (sh), 415mw 393w	298s,sp, 250s
$[Ru_3O_2(NH_3)_{10}(en)_2]Cl_7 \cdot 4H_2O$	840ms, 810ms, 760mw, 690w	590w, 530vw, 508mw	470w, 453vw, 405w	310mw, 283vw, 265m
$[Ru_3O_2(N^2H_3)_{10}\{[^2H_4]en\}_2]Cl_7 \cdot 4^2H_2O$	820 (sh), 797s, 705vw, 660vw, 640w	570vw, 490w	460mw, 395mw,br	320vw, 240m
Assignment	ν(RuO), $\rho(NH_3)$, $\rho(NH_2)$, and $\rho(CH_2)$	en or H_2O modes	ν(RuN)	ν(RuO), δ(ORuN), and δ(NRuN)

[a] Additional far-i.r. bands at 117, 93, and 58 cm^{-1}. [b] Additional far-i.r. bands at 123, 95, and 60 cm^{-1}.

In $[Ru_3O_2(NH_3)_{10}(en)_2]Cl_6$ there is again a linear N–Ru–O–Ru–O–Ru–N backbone [9] with bridging oxo-ligands [Ru(terminal)–O 1.891 Å, O–Ru(central) 1.850 Å]. Again there is octahedral co-ordination for each metal atom; the ammine groups (Ru–N 2.12—2.15 Å) are co-ordinated to the terminal ruthenium atoms and the two chelating 1,2-diaminoethane ligands (Ru–N 2.124 Å) to the central ruthenium atom. This latter RuN_4 plane has a dihedral angle of 45° relative to the two terminal RuN_4 entities [Figure 2(*b*)], so that the symmetry of the

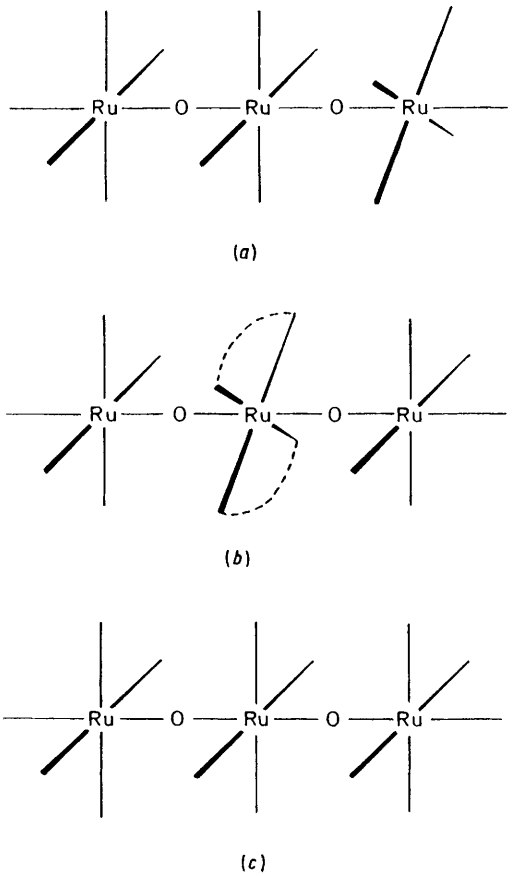

FIGURE 2 Possible skeletal symmetries of complex ions: (*a*) C_{4v}; (*b*) D_{2h}; and (*c*) D_{4h}

cation is D_{2h} (or D_{4h} if only the $Ru_3O_2N_{14}$ skeleton is considered).

Number of Bands.—All the bands reported in Tables 1—3 for the solutions are polarised (p *ca.* $\frac{1}{3}$) and are therefore assigned to totally symmetric modes of vibration as found in analogous species such as $[Ru_2OCl_{10}]^{4-}$.[11-13] Taking the 19 skeletal atoms of all these complexes (*i.e.* $Ru_3O_2N_{14}$) the expected 51 vibrational modes are distributed as follows: C_4 [Figure 2(*a*)] $\Gamma_{3N-6} = 14a + 9b + 14e$ (all Raman active; *a* polarised; *a*, *e* i.r. active); C_{4v} [Figure 2(*a*)] $\Gamma_{3N-6} = 12a_1 + 2a_2 + 5b_1 + 4b_2 + 14e$ (a_1 polarised; b_1, b_2, and *e* Raman active; a_1, *e* i.r. active); D_{2h} [Figure 2(*b*)] $\Gamma_{3N-6} = 9a_g + 3b_{1g} + 6b_{2g} + 6b_{3g} + 3a_u + 8b_{1u} + 8b_{2u} + 8b_{3u}$ (a_g polarised, b_{1g}, b_{2g}, b_{3g} Raman active; b_{1u}, b_{2u}, b_{3u} i.r. active); D_{4h} [Figure 2(*c*)] $\Gamma_{3N-6} = 6a_{1g} + a_{2g} + 3b_g + 2b_{2g} + 6e_g + a_{1u} + 6a_{2u} + b_{1u} + 3b_{2u} + 8e_u$ (a_{1g} polarised, b_{1g}, b_{2g}, e_g Raman active; a_{2u}, e_u i.r. active).

There will also be an additional totally symmetric mode associated with NH_3 rocking $\rho(N_{eq}H_3)$ in each case (see below).

The Raman spectra of the solids are similar to those of their solutions; the electronic transmission spectrum of $[Ru_3O_2(NH_3)_{14}][S_2O_3]_3 \cdot 4H_2O$ dispersed in a $Na_2[S_2O_3]$ disc is similar to that of $[Ru_3O_2(NH_3)_{14}]Cl_6 \cdot 4H_2O$ dispersed in a KCl disc and to that of the aqueous solution. Thus, it may well be that the symmetries of the cations found by *X*-ray studies on $[Ru_3O_2(NH_3)_{14}][S_2O_3]_3 \cdot 4H_2O$ and on $[Ru_3O_2(NH_3)_{10}(en)_2]Cl_6$ are retained in solution, *i.e.* C_4 (or perhaps C_{4v}) for $[Ru_3O_2(NH_3)_{14}]^{6+}$ and D_{2h} for $[Ru_3O_2(NH_3)_{10}(en)_2]^{6+}$. Since we observed 11 polarised bands in the Raman spectra of ruthenium red and of ruthenium brown and 13 in the spectra of the 1,2-diaminoethane analogues, this tentative conclusion appears to be borne out by the spectra. It is nevertheless simpler to confine most of the subsequent discussion of force constants and electronic spectra to the D_{4h} point group, since most of it would only be subject to minor qualification if one of the lower point groups were adopted.

Assignment of Bands.—The six normal modes for the a_{1g} polarised Raman active vibrations under D_{4h} symmetry are drawn in Figure 3, together with those for the i.r. active a_{2u} modes. Approximate descriptions of these modes are also given in Figure 3; Ru and N refer to terminal atoms and Ru′ and N′ to the central atoms in the cations, while N_{eq} and N_{ax} refer respectively to equatorial and axial atoms of the terminal RuN_5 units.

(*a*) *Raman spectra.* The following discussion concerns the spectrum of ruthenium red, but similar considerations apply equally well to the other three complexes and provide the basis for the suggested assignments in Tables 1—4.

The bands at 827 and 150 cm^{-1} are assigned to the predominantly metal–oxygen stretches ν_1 and ν_6. The ν_1 mode is mainly a movement of oxygen atoms along the Ru_3O_2 (*z*) axis and should, as observed, be much affected by ^{18}O substitution but little affected by ^2H or ^{15}N substitution. However, the ν_6 mode involves movement of the outer parts of the backbone rather than of the oxygen atom; ^2H and ^{15}N substitution will increase the effective masses of the terminal $Ru(NH_3)_5$ groups so that, as observed, ν_6 should be sensitive to such substitution but not to ^{18}O. These wavenumbers may be compared with those (887 and 256 cm^{-1}) for the asymmetric and symmetric Ru_2O stretches in $K_4[Ru_2OCl_{10}]$ [11,13] (in this complex, the Ru–O distance of 1.801 Å [14,15] is slightly less than that in ruthenium red, implying that the Ru–O bond in $[Ru_2OCl_{10}]^{4-}$ is slightly the stronger).

The other a_{1g} fundamentals principally concern the metal–ammine stretches $\nu_2(\nu RuN_{eq})$, $\nu_3(\nu Ru'N')$, and $\nu_4(\nu RuN_{ax})$ and the deformation $\nu_5(\delta ORuN_{eq})$. For comparison, ν(RuN) stretches are found in the 500—463 cm^{-1} range and δ(NMN) near 270 cm^{-1} in $[Ru^{III}(NH_3)_6]Cl_3$,[16] at 488—454 and 256—240 cm^{-1} respectively in

$[Ru^{III}(NH_3)_5Cl]Cl_2$,[17] and at 520—428 and 230 cm^{-1} respectively in $[Ru^{II}_2(N_2)(NH_3)_{10}]Cl_4$.[18] We suggest that the 413 cm^{-1} band, which is much affected by ^2H, ^{15}N, and ^{18}O substitution,* is the axial mode ν_4; the somewhat low wavenumber may be due to the *trans* position of these ammine groups to the oxo-ligands. Being an axial mode we would expect ν_4 to couple with the Ru–O stretching modes and thus to be sensitive to ^{18}O substitution. The 474 and 443 cm^{-1} bands are then good candidates for ν_2 and ν_3; as equatorial modes we expect little change on ^{18}O substitution but a large effect on ^2H and ^{15}N substitution, as observed. The lower wavenumber of ν_3 than ν_2 is consistent with the known lability of the central ammine groups in ruthenium red (*e.g.* ease of replacement by 1,2-diaminoethane [9]) relative to the terminal groups. The band at 274 cm^{-1}, being little affected by ^{18}O- but very sensitive to ^2H- and ^{15}N-substitution, is likely to be the deformation ν_5.

Assignments of the remaining bands on this simplified scheme now requires allowance to be made for the protons or the possible lower symmetry for the cations. The strong band at 742 cm^{-1} may well arise from a symmetric $\rho(N_{eq}H_3)$ rock, which occurs at 788 cm^{-1} for $[Ru(NH_3)_6]Cl_3$.[16] It drops to 615 cm^{-1} on deuteriation {611 cm^{-1} in $[Ru(N^2H_3)_6]Cl_3$ [16]}; some coupling to the Ru–O stretch is apparent since it is sensitive to ^{18}O substitution. No positive assignments can be offered for the 370 cm^{-1} band or the weak 545 cm^{-1} band; they are not likely to arise from co-ordinated water brought about by possible aquation of the complex, since they are present in spectra of the solids as well as in solutions containing concentrated ammonia.

These resonance Raman spectra are notable for their lack of overtones, features which are very apparent in such spectra of binuclear oxo-bridged species.[10-13] One possible explanation is that *B*-term scattering is dominant. However, this would require vibronic coupling by the totally symmetric modes of the resonant electronic transition to the one next lowest in energy (at *ca.* 26 100 cm^{-1}). This band is very weak, though, and is therefore unlikely to give rise to a significant *B* term. A more plausible interpretation of the lack of overtones is the occurrence of only a small displacement along each totally symmetric normal co-ordinate in the resonant electronic state, giving rise to *A*-term intensity enhancement for fundamentals only. Such a situation is common in systems where the normal co-ordinates are combinations of several symmetry co-ordinates, *e.g.* metalloporphyrins, $[Pd_3(CNMe)_8][PF_6]_2$ and $[Pd_3(CNMe)_6(PPh_3)_2][PF_6]_2$,[19] as well as for the dinitrogen-bridged species $ClRe(PMe_2Ph)_4$–N=N–$MoCl_4$–N=N–Re–$(PMe_2Ph)_4Cl$.[20]

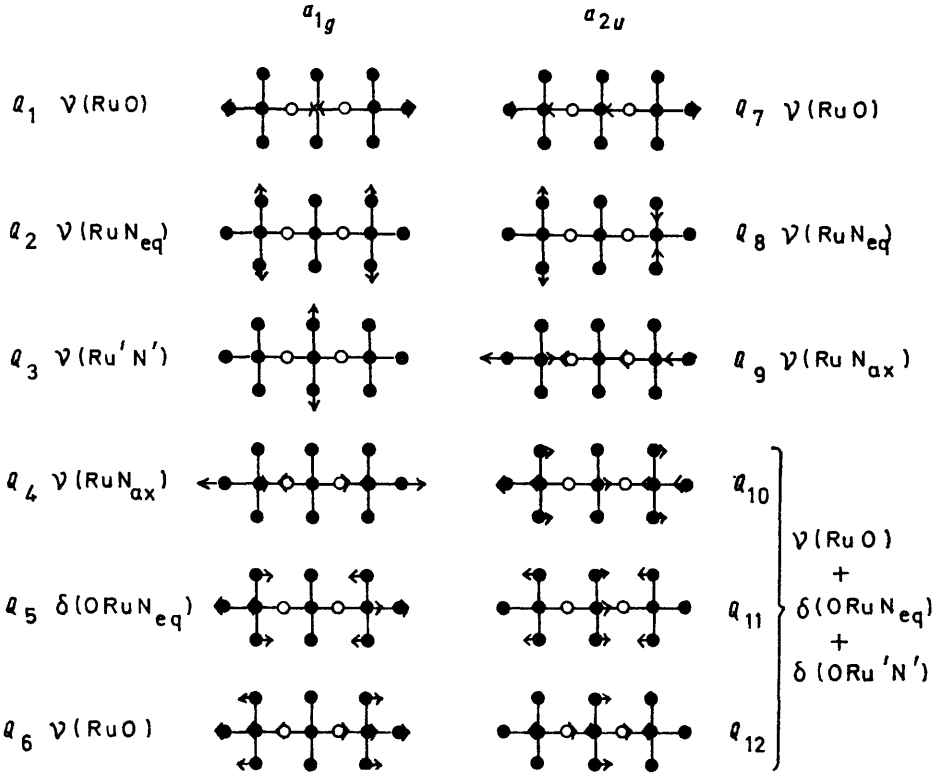

FIGURE 3 The a_{1g} and a_{2u} normal modes for $[Ru_3O_2(NH_3)_{14}]^{6+}$, assuming D_{4h} symmetry. Note, ν(RuO) here implies stretching of both the Ru–O and the Ru'–O bonds

(b) Infrared spectra. These were measured for the normal and deuteriated forms of the solids, and are

* The observed sensitivity of the wavenumber of this band to the environment of ruthenium red in biological systems [7] could well arise from an end-on attachment of the $[Ru_3O_2(NH_3)_{14}]^{6+}$ ion to the bonding sites.

listed in Table 4. Some data on these species have already been given.[6] We agree with previous workers [4,6,21] that the band near 820 cm^{-1} is probably due to an Ru–O stretch, perhaps ν_7 (although other possibilities for this include bands down to 670 cm^{-1}), while the bands near 450 and 270 cm^{-1} are clearly due to Ru–N stretches and deformations respectively. In Table 4 we list tentative assignments for some of these bands.

Force Constant Calculations.—Ruthenium red. (*a*) *The a_{1g} modes.* Force-constant calculations were carried out for two reasons: to help in the assignment of the bands in the Raman and i.r. spectra and to explain the excitation profiles of the Raman bands in terms of the extent of mixing of the a_{1g} symmetry co-ordinates.

Owing to the uncertainty of the assignments of the i.r. bands and some of the Raman bands, it was necessary to use a simplified model, assuming D_{4h} symmetry, and initially to consider the four axial a_{1g} modes only. Thus the symmetry co-ordinates employed were S_1—S_4 where

$$S_1 = \frac{1}{\sqrt{2}} \Sigma \Delta r(\mathrm{Ru'O})$$

$$S_2 = \frac{1}{\sqrt{2}} \Sigma \Delta r(\mathrm{RuO})$$

$$S_3 = \frac{1}{\sqrt{2}} \Sigma \Delta r(\mathrm{RuN_{ax}})$$

$$S_4 = \frac{1}{4} [\Sigma\Delta\beta - \Sigma\Delta\alpha]$$

β and α are the angles $N_{ax}RuN_{eq}$ and $ORuN_{eq}$ respectively. The NH_3 ligands were taken as point masses giving rise to a G matrix of the form shown below where $\mu(O) = 1/m(O)$, $\mu(Ru) = 1/m(Ru)$, $\mu(NH_3) = 1/m(NH_3)$, and $\omega = 1/r(RuN_{eq})$. A general quadratic valence force field was assumed and the F matrix was as shown below.

$$\begin{bmatrix} \mu(O) & -\mu(O) & 0 & 0 \\ & [\mu(Ru) + \mu(O)] & -\mu(Ru) & 2\sqrt{2}\mu(Ru)\omega \\ & & [\mu(Ru) + \mu(NH_3)] & -2\sqrt{2}\mu(Ru)\omega \\ & & & [8\mu(Ru) + 2\mu(NH_3)]\omega^2 \end{bmatrix}$$

$$\begin{bmatrix} F_{11} & F_{12} & 0 & 0 \\ & F_{22} & F_{23} & F_{24} \\ & & F_{33} & F_{34} \\ & & & F_{44} \end{bmatrix}$$

F_{13} was taken to be zero since there is no common atom involved in the S_1 and S_3 symmetry co-ordinates, and F_{14} was also set equal to zero owing to the lack of a common bond in the S_1 and S_4 symmetry co-ordinates.

In terms of valence-bond force constants, the above F matrix elements are given by F_{11}—F_{34}.

$$F_{11} = f(\mathrm{Ru'O}) + f(\mathrm{Ru'O/Ru'O})$$
$$F_{22} = f(\mathrm{RuO})$$
$$F_{33} = f(\mathrm{RuN_{ax}})$$
$$F_{44} = \tfrac{1}{2}[f(\mathrm{ORuN_{eq}}) + f(\mathrm{N_{ax}RuN_{eq}})]r^2(\mathrm{RuN_{eq}})$$
$$F_{12} = f(\mathrm{Ru'O/RuO})$$
$$F_{23} = f(\mathrm{RuO/RuN_{ax}})$$
$$F_{24} = -\sqrt{2}f(\mathrm{RuO/ORuN_{eq}})r(\mathrm{RuN_{eq}})$$
$$F_{34} = \sqrt{2}f(\mathrm{RuN_{ax}/N_{ax}RuN_{eq}})r(\mathrm{RuN_{eq}})$$

In order to reduce the number of force constants, F_{34} was set equal to zero (on grounds of its likely smallness) and f(Ru'O) and f(RuO) were taken to be equal. This is a reasonable assumption to make since the Ru'–O and Ru–O bond lengths are very similar {1.848 and 1.854 Å respectively for $[Ru_3O_2(NH_3)_{14}][S_2O_3]_3$ [5] and 1.850 and 1.891 Å respectively for $[Ru_3O_2(NH_3)_{10}(en)_2]Cl_6$}.[9] For similar reasons f(Ru'O/Ru'O) was taken to be equal to f(Ru'O/RuO). Hence F_{11}, F_{22}, and F_{12} can be reduced effectively to one force constant by setting $F_{12} = nF_{11}$ and $F_{22} = F_{11} - F_{12}$. The calculated values of the wavenumbers of the four a_{1g} bands will then depend parametrically on the value chosen for n, the best fit being found for $n = 0.23$. Note that the normal modes have been numbered in the order of decreasing wavenumber (Figure 3), and therefore the numbering of these does not necessarily correspond to those of the symmetry co-ordinates.

From this analysis, the normal modes turn out to be made up of the following mixtures (in terms of the potential energy distribution).

	S_1	S_2	S_3	S_4
Q_1	56	44	1	0
Q_4	5	13	81	1
Q_5	0	24	0	76
Q_6	41	52	3	4

As can be seen, both the normal co-ordinates Q_1 and Q_6 show extensive mixing of the symmetry co-ordinates S_1 and S_2 (*cf.* ref. 22). Q_4 and Q_5 are closer to being pure forms of S_3 and S_4 respectively, but still contain significant contributions from S_2 and, to a lesser extent, S_1. The forms of these normal co-ordinates are shown in Figure 3. As suggested by the potential energy distribution, Q_4 and Q_5 can be described as Ru–N_{ax} stretching and O–Ru–N_{eq} bending modes respectively. Q_1 and Q_6 can both be described as a mixture of Ru'–O and Ru–O stretches, the former mode being an out-of-phase combination and the latter an in-phase combination. Thus Q_1 largely consists of movement of the oxygen atoms only, whereas Q_6 can be described as a breathing mode of the Ru–O–Ru'–O–Ru chain with the $Ru(NH_3)_5$ groups moving as a whole. As a result, the wavenumbers of ν_1 and ν_6 are widely different due to a mass effect (827 to 150 cm^{-1}). For completeness, the forms of Q_2 and Q_3 are also included but are of course pure forms of S_5 and S_6, that is the Ru–N_{eq} and Ru'–N' stretching modes respectively.

A similar analysis of the appropriate data was carried out for ruthenium brown, and for the two 1,2-diaminoethane analogues (Table 5), again on the assumption of D_{4h} symmetry. The potential energy distribution and normal co-ordinates showed no significant changes from those of ruthenium red in any case.

(*b*) *a_{2u} Modes.* By using the force fields obtained above, it is possible to predict the wavenumbers of the a_{2u} bands in the i.r. spectra of all four species. There are five axial a_{2u} symmetry co-ordinates, four corresponding to the a_{1g} ones plus one involving deformations of the

TABLE 5

Force constants and calculated wavenumbers * for ruthenium red, ruthenium brown, and their 1,2-diaminoethane analogues

	$[Ru_3O_2(NH_3)_{14}]^{6+}$	$[Ru_3O_2(NH_3)_{14}]^{7+}$	$[Ru_3O_2(NH_3)_{10}(en)_2]^{6+}$	$[Ru_3O_2(NH_3)_{10}(en)_2]^{7+}$
F_{11}/mdyn Å^{-1}	4.77	5.21	4.89	5.22
F_{22}/mdyn Å^{-1}	3.67	3.83	3.62	3.78
F_{33}/mdyn Å^{-1}	1.74	1.82	1.73	1.74
F_{44}/mdyn Å rad^{-2}	1.25	1.29	1.30	1.36
F_{12}/mdyn Å^{-1}	1.10	1.38	1.27	1.44
F_{23}/mdyn Å^{-1}	0.89	0.89	0.89	0.89
F_{24}/mdyn rad^{-1}	−0.83	−0.83	−0.83	−0.83
$\tilde{\nu}_1$/cm^{-1}	828 (827)	829 (829)	810 (810)	820 (820)
$\tilde{\nu}_4$/cm^{-1}	413 (413)	424 (424)	410 (410)	412 (412)
$\tilde{\nu}_5$/cm^{-1}	274 (274)	281 (281)	279 (279)	289 (289)
$\tilde{\nu}_6$/cm^{-1}	150 (150)	157 (157)	152 (152)	157 (157)

* Observed band wavenumbers are given in parentheses.

O–Ru′–N′ angles, together with one non-axial mode. [Note, that, if the symmetry co-ordinates are numbered S_7 to S_{12}, the only changes with respect to the axial modes in the G and F matrix elements, apart from those arising from the extra (ORu′N′ bending) co-ordinate, are that $G_{77} = \mu(O) + 2\mu(Ru)$ and $F_{77} = f(Ru'O) - f(Ru'O/Ru'O)$.] The wavenumbers of these a_{2u} modes have been calculated and the forms of the normal modes are included in Figure 3.

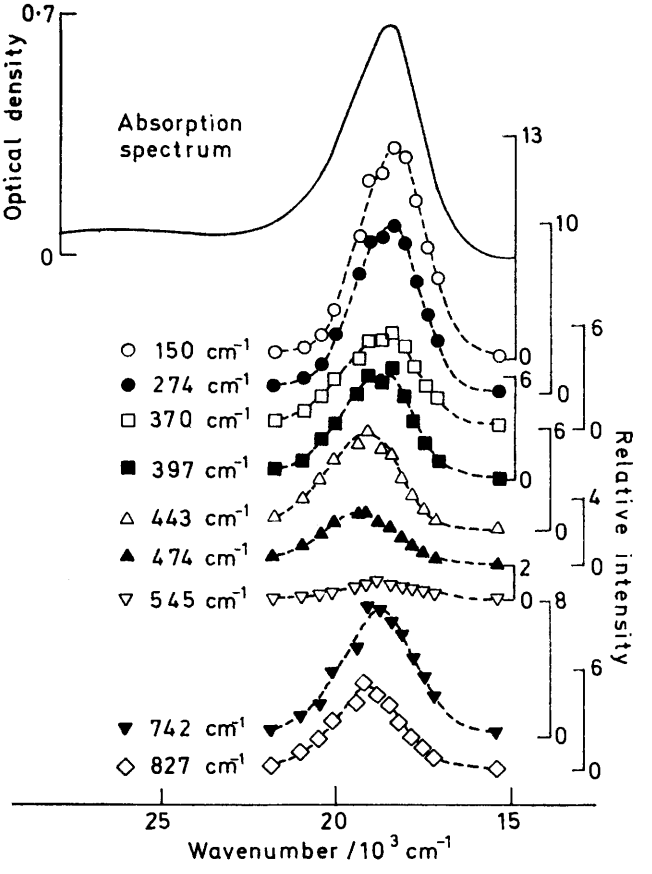

FIGURE 4 Excitation profiles for the totally symmetric (a_{1g}) bands of $[Ru_3O_2(NH_3)_{14}]^{6+}$, together with the electronic spectrum of the complex in aqueous solution

Discussion of force constants. Looking at Table 5, we see that the value of the Ru–O stretching force constant, f(RuO) (equal to F_{22}), for ruthenium red, ruthenium brown, and their 1,2-diaminoethane analogues is 3.67, 3.83, 3.62, and 3.78 mdyn Å^{-1}, respectively.* These relatively high values are consistent with the multiple bond character of the Ru–O bonds. These results also show that the Ru–O bond is stronger in the brown species than in the red species, a result which is consistent with a

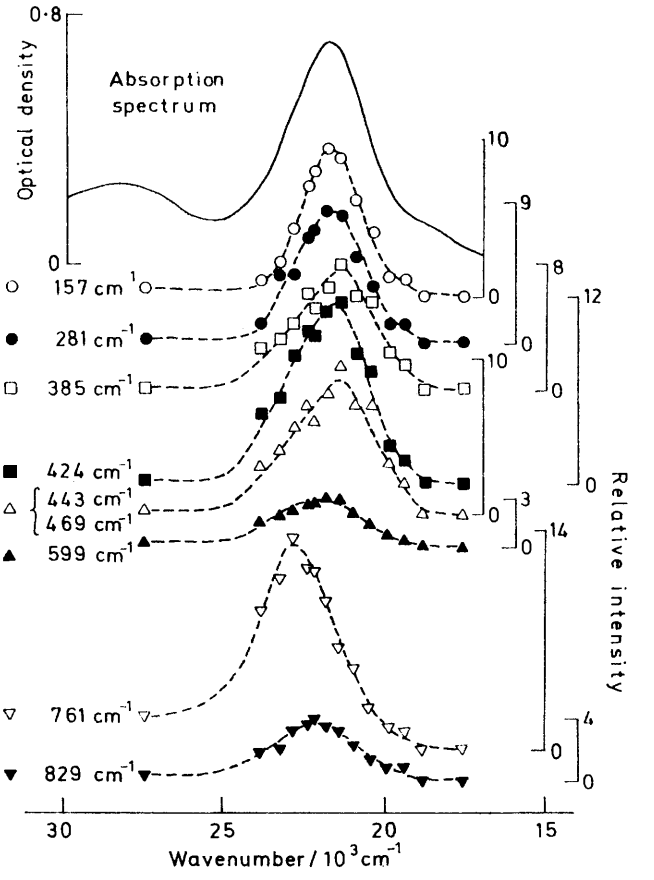

FIGURE 5 Excitation profiles of the a_{1g} bands of $[Ru_3O_2(NH_3)_{14}]^{7+}$, together with the electronic spectrum of the complex in aqueous solution

* Throughout this paper: 1 dyn = 10^{-5} N.

molecular-orbital scheme (see below) in which ruthenium red contains an extra antibonding electron in the Ru–O π system.

The values for the Ru–N_{ax} stretching force constants

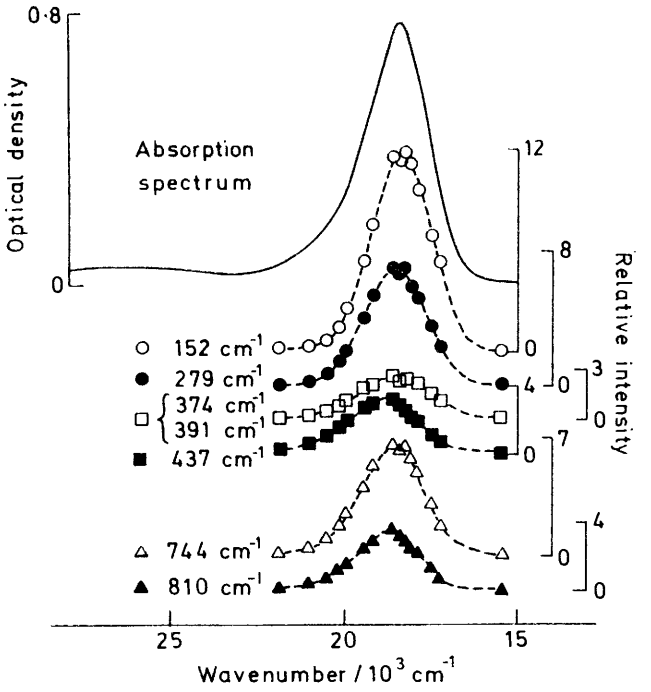

FIGURE 6 Excitation profiles of the a_{1g} bands of $[Ru_3O_2(NH_3)_{10}(en)_2]^{6+}$, together with the electronic spectrum of the complex in aqueous solution

are consistent with a normal Ru–N single bond and display the same trends as observed for the Ru–O stretching force constants.

Excitation Profiles and Electronic Spectra.—The excitation profiles of the bands in the Raman spectra of all four ions in aqueous solution have been determined by reference to the intensity of the $\nu_1(a_1)$ band of potassium sulphate. The results are displayed, along with the electronic absorption spectra, in Figures 4—7.

As can be seen, the excitation profiles of all bands (with two exceptions) maximise close to the electronic absorption maxima, which for ruthenium red, ruthenium brown, and their 1,2-diaminoethane analogues lie at *ca.* 18 620, 21 790, 18 420, and 21 100 cm^{-1} respectively. The two exceptions are the strong bands of ruthenium brown and its 1,2-diaminoethane analogue lying at 761 and 754 cm^{-1} respectively whose excitation profiles maximise some 1 000 cm^{-1} higher than the electronic maxima. The reason for this is uncertain.

A molecular-orbital scheme for ruthenium red is given in Figure 8. An eclipsed, D_{4h}, structure has been assumed and only the *d* orbitals of ruthenium atoms and the p_x and p_y orbitals of oxygen atoms have been considered. Our scheme is similar to that given by Earley and Fealey [6] for a 45°-twisted D_{4h} structure except that we have placed the $e_u(\pi^*)$ orbital at higher energy and have described it as antibonding rather than non-bonding.

The distribution of the 22 valence π electrons of the cation in the ground state, $Ru^{III}(d^5)O(p^4)Ru^{IV}(d^4)O(p^4)Ru^{III}(d^5)$, is indicated in Figure 8. Although the cation is strictly mixed valent in both the ground (*cf.* Mössbauer evidence) [23] as well as the excited states, no attempt has been made to position the Ru^{III} and Ru^{IV} orbitals at different energies; such a refinement to the molecular-orbital diagram was not considered justified by the present level of sophistication of the discussion, bearing in mind the degree of uncertainty as to the precise geometry of the cation in solution. Moreover, the displacement of the oxygen atoms away from the exact bridging position towards the central ruthenium atom (consistent with the view that this atom is in the higher

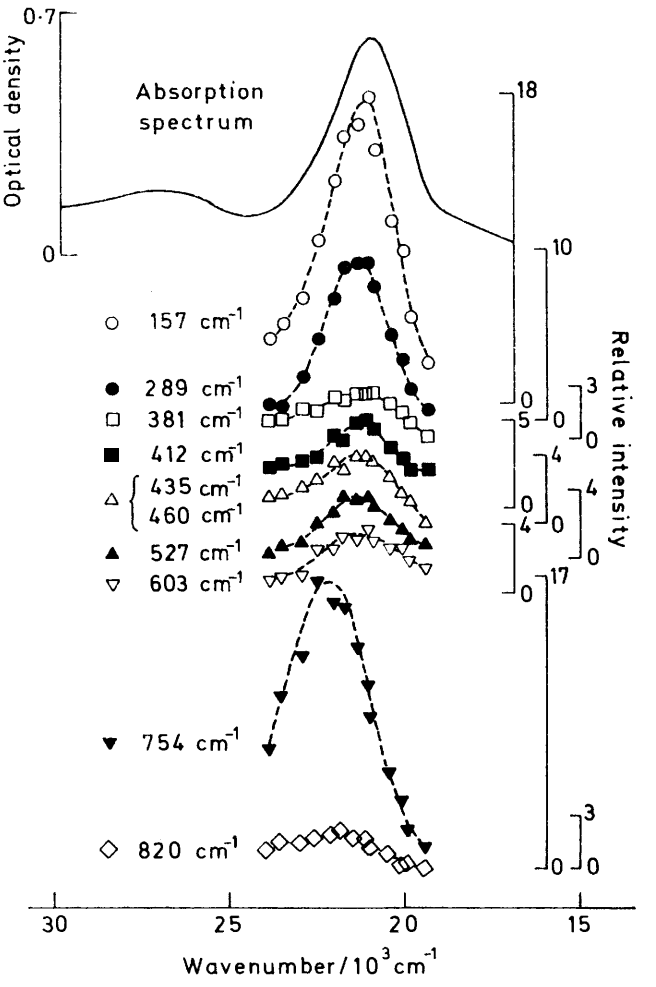

FIGURE 7 Excitation profiles of the a_{1g} bands of $[Ru_3O_2(NH_3)_{10}(en)_2]^{7+}$, together with the electronic spectrum of the complex in aqueous solution

oxidation state) is only very slight (0.20 Å) in the 1,2-diaminoethane-substituted complex.[9]

For ruthenium red, which has a ground-state configuration of $(e_g^b)^4(e_u^b)^4(b_{2g}^b)^2(b_{1u})^2(b_{2g}^*)^2(e_g)^4(e_u^*)^4(e_g^*)^0$, we assign the resonant electronic transition as

$e_g^* \leftarrow e_u^*$, $^1A_{2u} \leftarrow {}^1A_{1g}$ which is dipole-allowed *via* an A_{2u} component in z-polarisation (consistent with the observed depolarisation ratios of *ca.* $\frac{1}{3}$ for the a_{1g} bands on resonance).[24] Other possibilities are that the electron is transferred from a b_{2g}, b_{1u}, or e_g orbital but, of these, only the $e_g^* \leftarrow b_{1u}$, $^1E_u \leftarrow {}^1A_{1g}$ transition is allowed, and then only in x,y-polarisation. The same conclusions are reached for the 1,2-diaminoethane analogue of ruthenium red (assuming a staggered structure) where the transformation of a b_{2g} orbital to a b_{1g} orbital brought about by the 45° rotation of the $Ru'N_4'$ unit has no significant effect on these conclusions.

For ruthenium brown, which has a ground-state configuration of $(e_g^b)^4(e_u^b)^4(b_{2g}^b)^2(b_{1u})^2(b_{2g}^*)^2(e_g)^4(e_u^*)^3$, and its

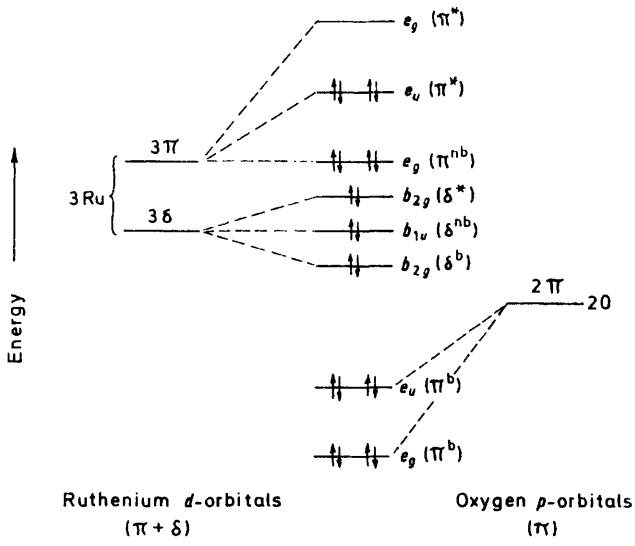

FIGURE 8 Molecular-orbital scheme for the π and δ system of ruthenium red, on the assumption of an eclipsed D_{4h} structure for the cation. The distribution of the 22 valence electrons of the cation in the ground state, $Ru^{III}(d^5)O(p^4)Ru^{IV}(d^4)O(p^4)$-$Ru^{III}(d^5)$, is indicated. The three δ orbitals in the complex are virtually degenerate owing to the large separation of the ruthenium atoms, and their energies relative to that of the $e_g(\pi^{nb})$ orbital are uncertain

1,2-diaminoethane analogue, we suggest that the resonant transition is $e_g^* \leftarrow e_u^*$, $^2E_g \leftarrow {}^2E_u$, which is allowed *via* both z- as well as x,y-polarised components, although dominated by the former since $p \approx \frac{1}{3}$ for the a_{1g} bands on resonance. Other possible transitions are $e_u^* \leftarrow b_{2g}$, $^2B_{2g} \leftarrow {}^2E_u$, $e_u^* \leftarrow e_g$, $^2E_g \leftarrow {}^2E_u$, or $e_g^* \leftarrow b_{1u}$, $^2X \leftarrow {}^2E_u$ (where $X = A_{1g}$, A_{2g}, B_{1g}, or B_{2g}). Such transitions, along with the $e_g^* \leftarrow b_{1u}$, $^1E_u \leftarrow {}^1A_{1g}$ transition of the red species, may be giving rise to the weaker absorption bands of ruthenium red, ruthenium brown, and their 1,2-diaminoethane analogues which lie at 26 100, 28 300, 26 500, and 27 000 cm^{-1} respectively.

Since the resonant electronic bands have been assigned to a transition involving the π^* orbitals of the Ru–O π system, one might expect only the Raman bands attributable to the Ru–O stretching modes to be enhanced. However, this is not the case since all the a_{1g} modes are enhanced. One possible explanation is that the resonant state is coupled to a second, charge-transfer state involving Ru–N as opposed to Ru–O bonding. Another, more likely explanation is that the symmetry co-ordinates are strongly mixed in the normal modes of the ground state, and that the extent of mixing is different in the resonant excited state. Force-constant calculations have shown this mixing is important for the ground state, and looking at Figure 3, we see that Q_1, Q_4, Q_5, and Q_6 all involve substantial amounts of Ru–O stretch. The equatorial ruthenium–nitrogen stretching modes Q_2 and Q_3 were not involved in our calculations since they have been treated as pure symmetry co-ordinates, but the introduction of the appropriate interaction force constants would easily allow for the mixing similar to that in Q_1, Q_4, Q_5, and Q_6.

The authors are indebted to the Science Research Council and to the University of London Intercollegiate Research Service for financial support. We thank Johnson, Matthey Ltd. for loans of platinum metals, and the Science Research Council for research studentships to two of us (J. R. C. and J. P. H.).

[9/1867 *Received*, 23*rd November*, 1979]

REFERENCES

1 A. Joly, *Compt. rend.*, 1892, **115**, 1299.
2 J. H. Luft, *Anat. Rec.*, 1971, **171**, 347.
3 K. C. Reed and F. L. Bygrave, *Biochem. J.*, 1974, **140**, 143.
4 J. M. Fletcher, B. F. Greenfield, C. J. Hardy, D. Scargill, and J. L. Woodhead, *J. Chem. Soc.*, 1961, 2000.
5 M. A. A. F. de C. T. Carrondo, W. P. Griffiith, J. P. Hall, and A. C. Skapski, *Biochim. Biophys. Acta*, 1980, **627**, 332.
6 J. E. Earley and T. Fealey, *Inorg. Chem.*, 1973, **12**, 323.
7 J. M. Friedman, D. L. Rousseau, G. Navon, S. Rosenfeld, P. Glynn, and K. B. Lyons, *Arch. Biochem. Biophys.*, 1979, **193**, 14.
8 J. E. Fergusson and J. L. Love, *Inorg. Synth.*, 1972, **13**, 210.
9 P. M. Smith, T. Fealey, J. E. Earley, and J. V. Silverton, *Inorg. Chem.*, 1971, **10**, 1943.
10 R. W. Stoddart, I. P. C. Spires, and K. F. Tipton, *Biochem. J.*, 1969, **114**, 863.
11 R. J. H. Clark, M. L. Franks, and P. C. Turtle, *J. Amer. Chem. Soc.*, 1977, **99**, 2473.
12 J. San Filippo, R. L. Grayson, and H. J. Sniadoch, *Inorg. Chem.*, 1976, **15**, 269.
13 J. R. Campbell and R. J. H. Clark, *Mol. Phys.*, 1978, **36**, 1133.
14 A. M. Mathieson, D. P. Mellor, and N. C. Stephenson, *Acta Cryst.*, 1957, **5**, 185.
15 J-P. Deloume, R. Faure, and G. Thomas-David, *Acta. Cryst.*, 1979, **B35**, 558.
16 W. P. Griffith, *J. Chem. Soc.* (*A*), 1966, 899.
17 M. W. Bee, S. F. A. Kettle, and D. B. Powell, *Spectrochim. Acta*, 1974, **A30**, 139.
18 M. W. Bee, S. F. A. Kettle, and D. B. Powell, *Spectrochim. Acta*, 1975, **A31**, 89.
19 R. J. H. Clark and C. Sourisseau, *Nouveau J. Chim.*, 1980, **4**, 287.
20 J. R. Campbell, R. J. H. Clark, and J. Dilworth, *J.C.S. Chem. Comm.*, 1980, in the press.
21 W. P. Griffith, *J. Chem. Soc.* (*A*), 1969, 2270.
22 J. R. Campbell and R. J. H. Clark, *J.C.S. Faraday II*, 1980, in the press.
23 C. A. Clausen, R. A. Prados, and M. L. Good, *Inorg. Nuclear Chem. Letters*, 1971, **7**, 485.
24 S. Hassing and O. S. Mortensen, in ' Advances in Infrared and Raman Spectroscopy,' eds. R. J. H. Clark and R. E. Hester, Heyden, London, 1980, vol. 6, p. 1.